

Breathing and wiggling motions in three-species laterally inhibitory systems

Mami Suzuki,¹ Takao Ohta,¹ Masayasu Mimura,² and Hideo Sakaguchi³

¹*Department of Physics, Ochanomizu University, Tokyo, 112 Japan*

²*Department of Mathematical Sciences, University of Tokyo, Tokyo, 153 Japan*

³*Department of Mathematics, Hiroshima University, Higashi-Hiroshima, 324 Japan*

(Received 24 May 1994; revised manuscript received 18 November 1994)

We study the layer dynamics in a coupled set of reaction-diffusion systems describing the interaction of one activator and two inhibitors. In some special limits, this set of equations is reduced to a Bonhoeffer–van der Pol–type excitable system or a model for electric glow discharge. Dynamics of layers is investigated by an interfacial approach and complementarily by computer simulations. By changing the parameters, these layers undergo several sustained oscillations such as breathing, wiggling, and quasiperiodic motions, which are due to the competition of two inhibitors and one activator.

PACS number(s): 47.35.+i, 02.30.-f, 82.20.Mj

I. INTRODUCTION

Pattern formation far from equilibrium has attracted increasing attention for more than 20 years. Extensive reviews can be found in Refs. [1,2]. The discovery of the Belousov-Zhabotinsky (BZ) reaction [3] was a landmark that both physicists and applied mathematicians began to study intensively this field. Curious patterns such as concentric and spiral waves [4] have been considered by analytical methods including approximate theories and computer simulations [5]. Recent experiments [6,7] of the ferrocyanide-iodate-sulphite reaction in gel reactors have realized spatially periodic motionless domains as a result of Turing instability [8].

The emergence of localized dissipative patterns has also been observed in semiconductor devices [9,10] and electric gas discharges [11,12]. In contrast to the chemical reactions, these localized domains undergo oscillatory instabilities. In fact, complicated motions of discharged domains as well as stationary periodic structures have been observed in both one and two dimensions. In an electric system some of the system parameters can be controlled in a tunable way. This is one of the advantageous features compared to chemical systems where, for instance, the reaction rates are not changed freely in some intervals. Thus the transition from one state to another in the electric systems can be investigated systematically.

From modeling view points, such pattern formation is described by a class of reaction-diffusion equations in the framework of activator-inhibitor systems. Throughout this paper we use the terminology of an activator and an inhibitor with the same meanings as widely accepted in the literature [13–15]. Originally the notion of activator and inhibitor was introduced in a two-component reaction-diffusion system. A substance is called an activator if it has a property of self-enhancement. The activator produces another substance that is called an inhibitor if it tends to suppress the growth of the activator. An example will be given below in Eqs. (1.3). A remarkable property of the system is that if the diffusion of the

activator is small compared to that of the inhibitor, a motionless localized solution [16] and/or a spatially periodic solution [14,17] can be formed. This is due to the Turing instability of a homogeneous steady state. It is remarked that the bifurcation is not necessarily supercritical. Depending on the nonlinearity of the system, a spatially periodic solution can appear as a subcritical bifurcation in a monostable state where a homogeneous solution is linearly stable. In the opposite limit such that the diffusion of the inhibitor is large, the system in a monostable condition exhibits a stably propagating pulse solution [18,19]. It is well known that the simplified model equation for the BZ reaction belongs to a one-inhibitor–one-activator system [20].

Recently it turns out that one has to consider an activator-inhibitor system with multiple components. For instance, the pattern dynamics in the electronic devices and glow discharge mentioned above is modeled by a two-inhibitor–one-activator system. See the transformation of Eqs. (1.2) to Eqs. (1.5) below. More generally, the interaction of multiple species of activators and inhibitors is often observed in population dynamics. One typical example is a population model system of N predator species and M prey species, both of which move by diffusion. These are basically described by

$$\frac{\partial u_i}{\partial t} = d_i \Delta u_i + f_i(u, v) u_i \quad (i = 1, 2, \dots, M), \quad (1.1a)$$

$$\frac{\partial v_j}{\partial t} = d_j \Delta v_j + g_j(u, v) v_j \quad (j = 1, 2, \dots, N), \quad (1.1b)$$

where $u = (u_1, u_2, \dots, u_M)$ and $v = (v_1, v_2, \dots, v_N)$ are population densities of the prey species and the predator species. The constants d_i and d_j are diffusion rates of u_i and v_j . The functions f_i and g_j are the growth rates of u_i and v_j , which possess prey and predator mechanisms, respectively. The readers should refer to [21] for specific forms of nonlinearities f_i and g_j .

Theoretical work on pattern dynamics arising in activator-inhibitor systems (1.1) has been intensively investigated from both theoretical and numerical

viewpoints [2,5,22]. However, most of them are restricted to two-component systems ($M=N=1$) and, as far as we know, there have been few attempts [23,24] to approach more multicomponent systems [25,26].

As the first step to theoretically understand such multicomponent systems, we propose one-dimensional reaction-diffusion equations that describe the interaction of two inhibitors ($N=2$) and one activator ($M=1$). The model equations take the following form for the activator u and the two inhibitory variables v and w with a sufficiently small positive constant ε :

$$\varepsilon \frac{\partial u}{\partial t} = \varepsilon^2 \frac{\partial^2 u}{\partial x^2} + f(u) - v - w + k, \quad (1.2a)$$

$$a(1-q) \frac{\partial v}{\partial t} = \frac{\partial^2 v}{\partial x^2} + r(1-s)u - v, \quad (1.2b)$$

$$aq \frac{\partial w}{\partial t} = rs \langle u \rangle - w, \quad (1.2c)$$

where $f(u)$ is N shaped such as $f(u)=u-u^3$ and $f(u)=-u-H(u)$ with $H(u)=\pm 1$ for $u \geq 0$. The parameters a , k , q , r , and s are constants. The angular brackets $\langle \rangle$ mean the spatial average.

Because $f(u)$ is an N -shaped function, one may expect that Eqs. (1.2) admit a spatially nonuniform stationary solution for suitable values of k , r , and s , which connects two uniform solutions, say, u^+ and u^- . The width of the boundary between u^+ and u^- is of order ε and is very small for small values of ε . Hereafter we call this thin boundary an internal layer or an interface. The motion of internal layers characterize the time evolution of the spatial pattern. For this reason, we are interested in the dynamics of internal layers and especially the stability of stationary internal layers by using a singular limit analysis as ε tends to zero, which is called an interfacial approach [27].

Let us first briefly explain Eqs. (1.2). When $s=0$, Eq. (1.2c) is decoupled with Eqs. (1.2a) and (1.2b) and the solution w vanishes asymptotically. Thus it turns out that Eqs. (1.2a) and (1.2b) reduce to the one-inhibitor-one-activator system with the Bonhoeffer-van der Pol kinetics:

$$\varepsilon \frac{\partial u}{\partial t} = \varepsilon^2 \frac{\partial^2 u}{\partial x^2} + f(u) - v + k, \quad (1.3a)$$

$$\alpha \frac{\partial v}{\partial t} = \frac{\partial^2 v}{\partial x^2} + ru - v, \quad (1.3b)$$

with $\alpha=a(1-q)$. This reduced system (1.3) has been investigated by singular perturbation techniques and an interfacial approach [2,16,17,27-32]. Koga and Kuramoto [16] predicted that a motionless localized solution of Eqs. (1.3) undergoes a breathing motion when α is sufficiently large. Later, the existence of a breathing motion was proved in a mathematically rigorous manner [28]. Ohta, Mimura, and Kobayashi [29] have extended these one-dimensional results to higher dimensions. Oscillations of interacting domains in a spatially periodic solution have also been exploited [17]. One of the conclusions obtained in Ref. [17] is that a coherent in-phase oscillation of domains is the primary mode of oscillation in Eqs. (1.3).

Problems similar to those considered in Refs. [16,28,29] have been investigated independently by Kerner and Osipov [30,31]. Quite recently, Ikeda and Nishiura [32] have analyzed the oscillatory behavior in further detail.

In the opposite special case of $s=1$, Eq. (1.2b) implies that $v(x,t)$ becomes asymptotically zero so that (u,w) becomes the so-called shadow system, which is also a one-inhibitor-one-activator system

$$\varepsilon \frac{\partial u}{\partial t} = \varepsilon^2 \frac{\partial^2 u}{\partial x^2} + f(u) - w + k, \quad (1.4a)$$

$$\beta \frac{\partial w}{\partial t} = r \langle u \rangle - w, \quad (1.4b)$$

with $\beta=aq$. The only difference between (1.3) and (1.4) is the different diffusivities of the inhibitors v and w . Equations (1.4) have also been considerably studied by an interfacial approach [33]. We note that the system exhibits no oscillatory behavior.

On the other hand, if we set $q=0$, Eqs. (1.2) are written as

$$\varepsilon \frac{\partial u}{\partial t} = \varepsilon^2 \frac{\partial^2 u}{\partial x^2} + f(u) - v - rs \langle u \rangle + k, \quad (1.5a)$$

$$a \frac{\partial v}{\partial t} = \frac{\partial^2 v}{\partial x^2} + r(1-s)u - v. \quad (1.5b)$$

A feature of this system is that the activator u is inhibited by not only v but also its own spatial average $\langle u \rangle$. Equations (1.5) are essentially identical to the model equations for glow discharge proposed by Radehaus *et al.* [34]. In a gas-discharge system, the activator u is the current density and the inhibitor v is the voltage drop across the gas gap. Here we do not describe the derivation of (1.5) for glow discharge because it is lengthy; for details see Ref. [34]. There they have shown by computer simulations that a localized solution of (1.5) exhibits a wiggling motion. When $s=1$ in (1.5), the system is decoupled so that Eq. (1.5a) reduces to a time-dependent Ginzburg-Landau equation if one sets $f(u)=u-u^3$.

From the above consideration, Eqs. (1.2) can be interpreted as follows. For arbitrarily fixed a and r , the parameter s implies the ratio of the inhibitor magnitude of v and w to an activator u , while q implies the dynamics ratio of v and w to u . Furthermore, the activator u diffuses so slowly compared to v and w and the diffusion constants of v and w are totally different in a sense that w diffuses infinitely fast.

The purpose of this paper is to study dynamics of internal layers in Eqs. (1.2) in order to understand how two inhibitors influence pattern dynamics of the activator and, in particular, from the stability viewpoint of equilibrium solutions, to consider how (1.2) is different from the one-inhibitor-one-activator system when the parameters are globally varied. What we would like to emphasize is that (1.2) exhibits not only breathing motion, which has already been obtained in a one-inhibitor-one-activator system, but also wiggling motion and, furthermore, very complicated oscillations such as quasiperiodic behavior.

As mentioned above, the model equations (1.2) are related, on the one hand, to BZ-like chemical reactions

and, on the other hand, to electric discharge. However, we do not intend to make a detailed comparison with the experimental results. We are mainly concerned with the global feature of the model and clarify the role of the inhibitors in the appearance of various types of oscillations.

The organization of this paper is as follows. In Sec. II we carry out computer simulations of Eqs. (1.2). Various domain motions are identified. In order to understand theoretically these dynamic behaviors of patterns, we derive, in Sec. III, an interface equation from (1.2), taking the limit $\epsilon \rightarrow 0$. The linear stability analysis of the interface equation of motion is performed in Sec. IV and the stability diagram of equilibrium solutions with spatially periodic structures is drawn. In Sec. V we carry out computer simulations of the interface equation of motion and compare those with the numerical results obtained in Sec. II for sufficiently small but not zero ϵ . Finally, we make concluding remarks and discussions in Sec. VI.

II. SIMULATIONS OF LAYER DYNAMICS

A. Interaction of two inhibitors and one activator

Before we treat the system (1.2), we should briefly mention how it can be derived from the two-inhibitor-one-activator system. The first system that we introduce is the three-component system for (u, v_1, v_2)

$$\frac{\partial u}{\partial t} = d \frac{\partial^2 u}{\partial x^2} + f(u) - c_1 v_1 - c_2 v_2 + k, \quad (2.1a)$$

$$\frac{\partial v_1}{\partial t} = d_1 \frac{\partial^2 v_1}{\partial x^2} + a_1 u - b_1 v_1, \quad (2.1b)$$

$$\frac{\partial v_2}{\partial t} = d_2 \frac{\partial^2 v_2}{\partial x^2} + a_2 u - b_2 v_2, \quad (2.1c)$$

where $f(u)$ has appeared in Eq. (1.2a). It is obvious to see that the kinetics in (2.1) is a straightforward extension of the well known Bonhoeffer-van der Pol kinetics because, when $d_1 = d_2 = d'$, $a_1 = a_2 = a$, $b_1 = b_2 = b$, $c_1 = c_2 = c$, and $g_1(u, v) = g_2(u, v) = au - bv$, (2.1) reduces to the essentially two-component system for u and v ,

$$\frac{\partial u}{\partial t} = d \frac{\partial^2 u}{\partial x^2} + f(u) - cv + k, \quad (2.2a)$$

$$\frac{\partial v}{\partial t} = d' \frac{\partial^2 v}{\partial x^2} + au - bv. \quad (2.2b)$$

By setting $d = \epsilon^2$, $c_1 = c_2 = 1$, $d_1 = 1/[a(1-q)]$, $a_1/d_1 = r(1-s)$, $b_1/d_1 = 1$, $d_2 = D/(aq)$, $Da_2/d_2 = rs$, and $aqb_2 = 1$, the set of equations (2.1) is rewritten in terms of $u, v = v_1$, and $w = v_2$ as

$$\frac{\partial u}{\partial t} = \epsilon^2 \frac{\partial^2 u}{\partial x^2} + f(u) - v - w + k, \quad (2.3a)$$

$$a(1-q) \frac{\partial v}{\partial t} = \frac{\partial^2 v}{\partial x^2} + r(1-s)u - v, \quad (2.3b)$$

$$aq \frac{\partial w}{\partial t} = D \frac{\partial^2 w}{\partial x^2} + rsu - w, \quad (2.3c)$$

where $a > 0$, $r > 0$, $0 < q < 1$, and $0 < s < 1$ are all con-

stants. Here we consider the situation where the diffusivity of u is so slow compared with those of v and w that we may assume ϵ to be sufficiently small. Furthermore, we assume that the diffusion rate D approaches infinity. Then, under the zero-flux boundary conditions, $w(x, t)$ becomes spatially homogeneous, say, $w(t)$ and, taking the spatial average of (2.3c) with respect to x , we obtain

$$aq \frac{\partial w}{\partial t} = rs \langle u \rangle - w, \quad (2.3d)$$

where $\langle u \rangle$ means the spatial average of u . Equations (2.3a), (2.3b), and (2.3d) constitute the model system (1.2) demonstrated in the Introduction.

B. Numerical simulations

In this subsection, we numerically solve the system (2.3a), (2.3b), and (2.3d) with sufficiently small $\epsilon > 0$ in a finite interval $0 < x < L$ under the zero-flux boundary conditions at $x = 0$ and L and show what kind of asymptotic states appears in the system, depending upon the values of q and s . The other parameters are suitably fixed to be $\epsilon = 0.02$, $k = 0.5$, $a = 600$, $r = 1.5$, $L = 1.5$, and $f(u) = u - 0.008u^3$.

In our simulations, we restrict our consideration to the situation where only two internal layers exist in the interval in such a way that $u(x, t)$ exhibits a one-pulse solution as in Fig. 1. Here we simply call such an equilibrium solution with internal layers an equilibrium solution without confusion. We note that any solution with no reflection symmetry with respect to $x = L/2$ is spatially periodic with the period $2L$ because of the reflection property at the system boundaries with zero-flux boundary conditions.

We demonstrate the asymptotic states of the solutions in the (q, s) square region. These are basically classified into five patterns depending on the values of q and s , as in Fig. 2: (i) equilibrium state, E ; (ii) breathing (in-phase) motion, B ; (iii) wiggling (antiphase) motion, W ; (iv) quasi-periodic motion, Q ; (v) another complicated pattern, C . In Fig. 3 we illustrate schematically the breathing and wiggling motions of domains. The existence of these pat-

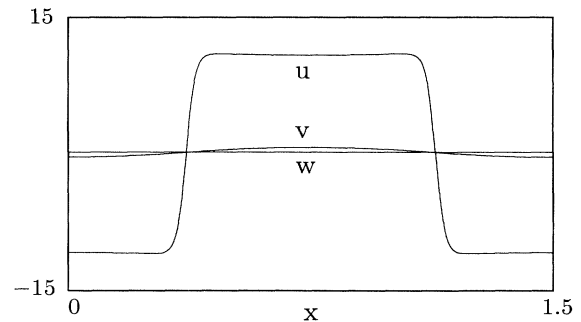


FIG. 1. Equilibrium solution obtained by simulations.

terns E , B , W , Q , and C clearly indicates occurrences of two different types of bifurcations. More qualitatively speaking, we have the following classification: (1) for fixed q to be close or equal to 1, all equilibrium solutions are always stable for any $0 < s < 1$; (2) for fixed s to be close to 1, all equilibrium solutions are always stable for any $0 < q < 1$; (3) for fixed s to be close or equal to 0, when q decreases from 1 to 0, the equilibrium solution becomes unstable through an in-phase Hopf bifurcation primarily; (4) for fixed q to be intermediate in $0 < q < 1$, when s decreases, the equilibrium solution becomes unstable through an in-phase Hopf bifurcation (occurrence of breathing motions of layers); (5) for fixed q to be close or equal to 0, when s decreases, the equilibrium solution be-

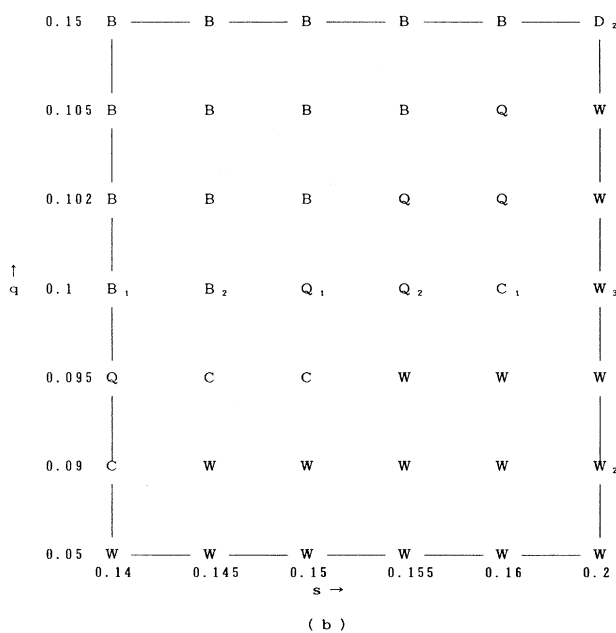
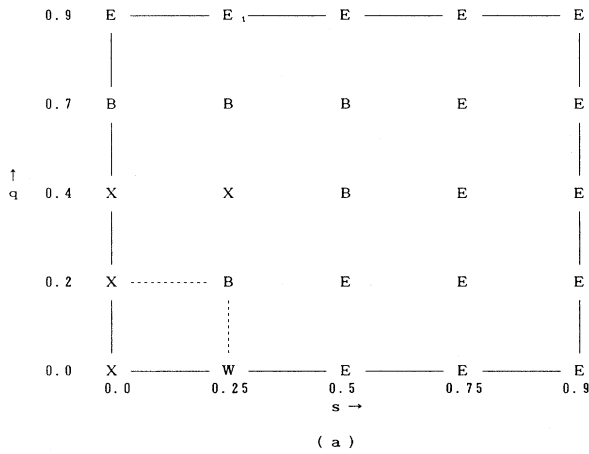


FIG. 2. Phase diagram obtained by simulations of Eqs. (2.3) in the region (a) for $0 < q < 0.9$ and $0 < s < 0.9$ and (b) for $0.05 < q < 0.15$ and $0.14 < s < 0.2$.

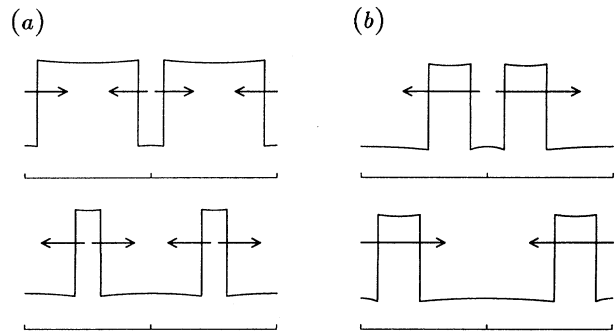


FIG. 3. Two kinds of motion of domains: (a) breathing and (b) wiggling motions.

comes unstable through an antiphase Hopf bifurcation (occurrence of wiggling motions of layers); (6) there are some values of q and s such that a double Hopf bifurcation occurs, that is, in- and antiphase bifurcations simultaneously occur.

We should give here some remarks on these results. When $s = 0$ [case (3)], the system for (u, v) is decoupled with the equation for w and reduces to the well known one-activator-one-inhibitor system as given by Eqs. (1.3). When q decreases, in-phase instability primarily occurs. In fact, as shown in Ref. [17], this system prefers in-phase

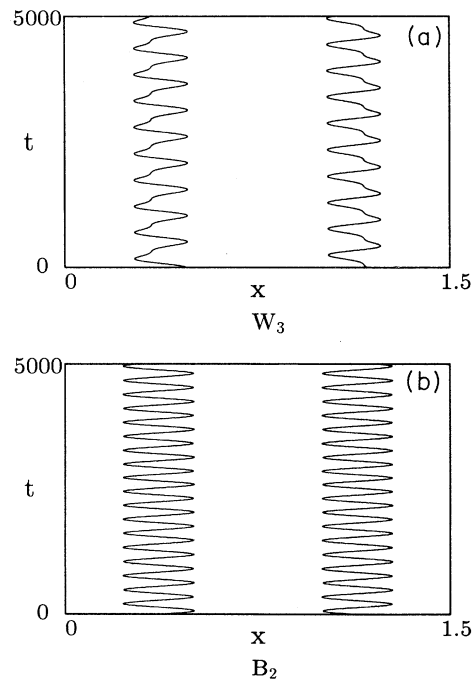


FIG. 4. Motion of interfaces in the space- (horizontal) time (vertical) plane: (a) wiggling motion for $q = 0.1$ and $s = 0.2$ and (b) breathing motion for $q = 0.1$ and $s = 0.145$.

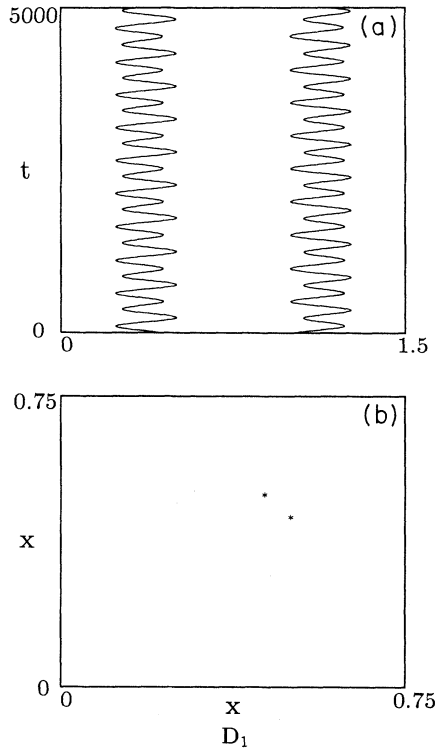


FIG. 5. (a) Period doubling of breathing motion for $q=0.15$ and $s=0.25$. The meaning of the lines is the same as in Fig. 4. (b) Lorentz plot.

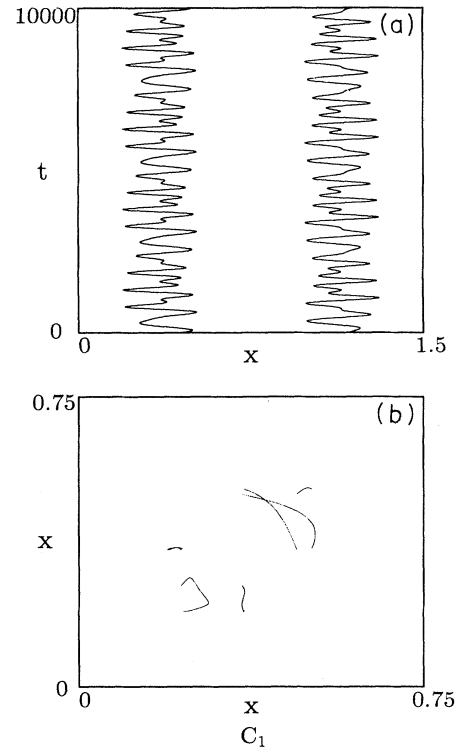


FIG. 7. (a) Chaotic motion of domain for $q=0.15$ and $s=0.16$ and (b) its Lorentz plot.

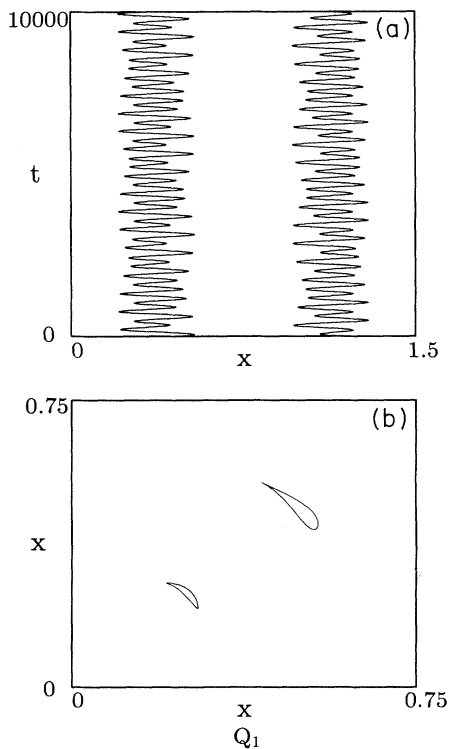


FIG. 6. (a) Quasiperiodic motion of domain for $q=0.15$ and $s=0.15$ and (b) its Lorentz plot.

oscillation. For case (6), more complicated oscillations are generally expected around the double Hopf bifurcation point. In fact, as will be shown below, quasiperiodic oscillations can be found.

Figure 2(a) shows the phase diagram of various oscillating modes obtained by simulations. The region $0.05 < q < 0.15$ and $0.14 < s < 0.2$ was explored in further detail in Fig. 2(b). The actual domain motions are summarized in Figs. 4–7 where the trajectories of the interfaces are plotted in the space-time plane. Figure 4(a) is a wiggling motion for $q=0.1$ and $s=0.2$ while Fig. 4(b) shows a breathing motion for $q=0.1$ and $s=0.145$. A period doubling of a breathing motion is shown in Fig. 5(a), where $q=0.15$ and $s=0.25$. In order to confirm the period doubling we have plotted a Lorentz map in Fig. 5(b). For smaller values of q , more complicated motions appear between the breathing and wiggling oscillations. A typical example of a quasiperiodic motion is given for $q=0.1$ and $s=0.15$ in Fig. 6(a) together with the Lorentz plot in Fig. 6(b). For slightly larger values of s , the Lorentz map does not exhibit a closed orbit but becomes pieces of broken lines. We call this a chaotic oscillation. Figure 7 shows examples for $q=0.1$ and $s=0.16$.

III. INTERFACE EQUATION OF MOTION

As mentioned in Introduction, the sufficiently small parameter ϵ in Eq. (1.2a) plays a role of a measure of a layer width that separates two qualitatively different sub-

domains, say, L_+ , where $u > 0$, and L_- , where $u < 0$, as in Fig. 1. The former is often called an excited domain, while the latter is a rest domain. Therefore when ϵ tends to zero, we may regard internal layers as structureless geometrical interfaces in such a way that time evolution of the spatial pattern is described by the dynamics of either excited or rest domains, which is given by the motion of interfaces between them.

For the explicit computation, we specify the function $f(u)$ as a piecewise linear form

$$f(u) = \begin{cases} -u - 1 & \text{for } u < 0 \\ -u + 1 & \text{for } u > 0. \end{cases} \quad (3.1)$$

Note that this definition of $f(u)$ is different from the previous one [17,29].

First, we assume that an equilibrium solution with two internal layers with width $O(\epsilon)$ has symmetry with respect to $x = 0$. Note here that the origin of the x coordinate is different from that in Sec. II. Actually the origin is shifted by the factor $L/2$. Therefore, if one extends this solution in the whole interval R under the reflection with zero-flux boundary conditions, one obtains the spatially periodic equilibrium solution with the period L . By taking the limit $\epsilon \rightarrow 0$, this solution is discontinuous at the interfaces, say, $x = \pm l/2$, in such a way that the period and the excited domain width are respectively L and l . For a general domain configuration, we introduce the right (left) interface position X^+ (X^-) such that $u(X^\pm, t) = 0$ for $x = X^\pm$. It turns out that $X^\pm = \pm l/2$ for the equilibrium solution. It should be noted that when the domain undergoes wiggling motion, the period is $2L$ because, in an antiphase oscillation, adjacent domains os-

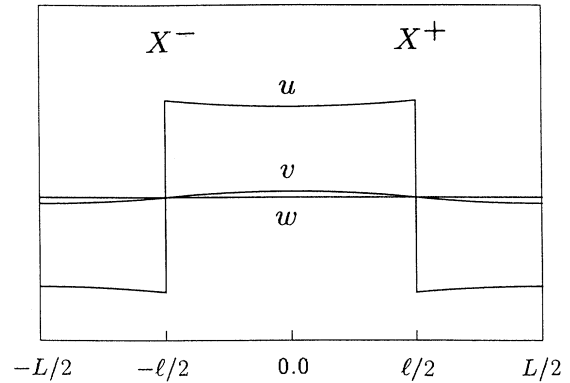


FIG. 8. Equilibrium solution of Eqs. (1.2) in the limit $\epsilon \rightarrow 0$.

cillate with a phase difference π . Then the spatial average $\langle u \rangle$ is given as

$$\langle u \rangle = \frac{1}{2L} \int_0^{2L} dx u(x, t). \quad (3.2)$$

Now we express Eqs. (1.2b) and (1.2c) for v and w in terms of X^\pm . In the limit $\epsilon \rightarrow 0$, Eq. (1.2a) can be solved as

$$u = -v - w + k + H(u), \quad (3.3)$$

where $H(u) = 1$ for $u > 0$ and -1 for $u < 0$. In terms of the interface positions X^+ and X^- as in Fig. 8, $H(u)$ can be explicitly written as

$$H(u) = \theta(x - X^+) \theta(-x + X^-) + \theta(x - L + X^+) \theta(-x + L - X^-) - \theta \left[x + \frac{L}{2} \right] \theta(-x + X^-) - \theta(x - X^+) \theta(-x + L - X^+) - \theta(x - L + X^-) \theta(-x + \frac{3}{2}L), \quad (3.4)$$

where $\theta(x) = 1$ for $x > 0$ and 0 for $x < 0$. The spatial average $\langle u \rangle$ is given from (3.3) and (3.4) by

$$\langle u \rangle = -\langle v \rangle - w + k + \frac{2}{L}(X^+ - X^-) - 1. \quad (3.5)$$

By using the Fourier expansion of the variable v ,

$$v(x, t) = C_0(t) + \sum_{n=1}^{\infty} C_n(t) \cos \left[\frac{\pi n}{L} \left[x - \frac{L}{2} \right] \right], \quad (3.6)$$

Eq. (1.2b) can be written in terms of the Fourier components $C_n(t)$ ($n = 0, 1, \dots$). From (3.5) and the fact that $\langle v \rangle = C_0$, it follows that

$$a(1-q) \frac{dC_0}{dt} = -r(1-s) \left[C_0 + w - k + 1 - \frac{2}{L}(X^+ - X^-) \right] - C_0. \quad (3.7a)$$

Equation for $n \neq 0$ is given from (1.2b) and (3.4) by

$$a(1-q) \frac{dC_n}{dt} = - \left[1 + r(1-s) + \left[\frac{\pi n}{L} \right]^2 \right] C_n + r(1-s) B_n, \quad (3.7b)$$

where

$$B_n = \frac{8}{\pi n} \sin \left[\frac{\pi n}{2L}(X^+ - X^-) \right] \cos \left[\frac{\pi n}{2L}(L - X^+ - X^-) \right]. \quad (3.7c)$$

Similarly one may write Eq. (1.2c) as

$$aq \frac{dw}{dt} = -rs \left[C_0 + w - k + 1 - \frac{2}{L}(X^+ - X^-) \right] - w. \quad (3.8)$$

We now derive the equations for the interface positions X^+ and X^- . In the limit $\epsilon \rightarrow 0$, we could expect that the spatial variation of v is weak compared to that of u . Therefore we may regard v in Eq. (1.2a) as a constant independent of x [17,29]. Actually, when we are concerned with the motion of X^\pm , we may set $v(x, t) = v(X^\pm, t) = v_I^\pm$. The value of v at the interface is given from (3.6) by

$$v_I^\pm = C_0(t) + \sum_{n=1}^{\infty} C_n(t) \cos \left[\frac{\pi n}{L} \left(X^\pm - \frac{L}{2} \right) \right]. \quad (3.9)$$

Furthermore, the effect of other domain boundaries is negligible since $\epsilon/l \ll 1$. Thus the time variation of X^+ can be obtained from an isolated interface as shown in Fig. 9. Under these conditions, a steady propagating solution of (1.2a) can be readily obtained [35]. The velocity is given by

$$c(V) = - \frac{2V}{\{(1+V)(1-V)\}^{1/2}}, \quad (3.10)$$

with $V = v_I^\pm + w - k$. Thus one obtains the equations for X^\pm

$$\frac{dX^\pm}{dt} = \pm c(V). \quad (3.11)$$

In this way one arrives at the complete form for the interface equations of motion (3.7)–(3.11) for the unknown variables [$X^\pm(t), v(x, t)$].

Finally, we make a remark about the nonlinear function $f(u)$ defined by (3.1). One can make a transformation to the system with the previous definition [17,29] $f(u) = -u$ for $u < 0$ and $-u + 1$ for $u > 0$ by the following replacements: $u \rightarrow 2u$, $v \rightarrow 2v$, $w \rightarrow 2w$, and $k \rightarrow 2k + 1$.

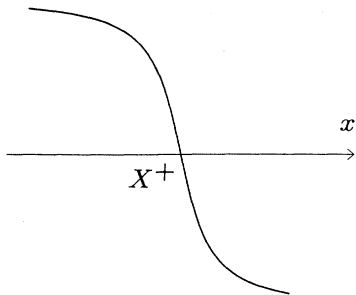


FIG. 9. Spatial variation of the activator u inside the internal layer (interface).

IV. LINEAR STABILITY OF THE LAYER STRUCTURE

First we solve the stationary problem for the interface equation obtained in Sec. III. From (3.11) one has $c(V) = 0$ so that (3.10) implies

$$k = v_I^\pm + w. \quad (4.1)$$

The equilibrium values of w and C_0 are obtained from (3.7a) and (3.8) with $X^\pm = \pm l/2$, respectively, as

$$w = \frac{rs}{1+r} \left[k - 1 + \frac{2l}{L} \right] \quad (4.2)$$

and

$$C_0 = \frac{r(1-s)}{1+r} \left[k - 1 + \frac{2l}{L} \right]. \quad (4.3a)$$

The equilibrium solution of the Fourier components $C_n^{(0)}$ for $n \neq 0$ is given from (3.7b) by

$$C_n^{(0)} = \frac{8}{\pi n} \frac{r(1-s)}{1+r(1-s) + \left[\frac{\pi n}{L} \right]^2} \sin \left[\frac{\pi n}{2L} l \right] \cos \frac{\pi n}{2}. \quad (4.3b)$$

Note that this is finite only for even integers of n , i.e., $n = 2m$. Substituting (4.2) and (4.3) into (4.1) and some manipulation yield

$$k = -r \left[1 - \frac{2l}{L} \right] + (1+r)\gamma \sum_{m=1}^{\infty} \frac{2}{\pi m} \frac{1}{1 + \gamma + \left[\frac{2\pi m}{L} \right]^2} \times \sin \left[\frac{2\pi m}{L} l \right], \quad (4.4)$$

where $\gamma = r(1-s)$. By solving this with the summation truncated at $m = 100$, the domain width l is given, depending on k . We thus find that equilibrium solutions are obtained as a function of k , r , and s . The result is shown in Fig. 10. Especially when $l/L = \frac{1}{2}$ it is readily seen that

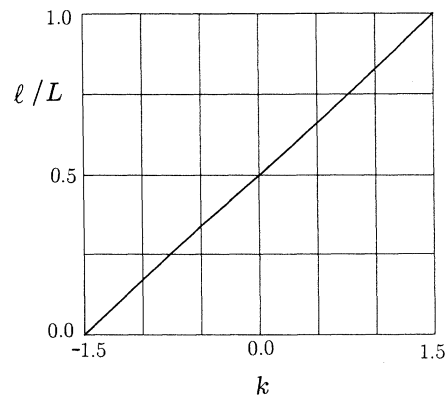


FIG. 10. Scaled domain width l/L as a function of k for $r = 1.5$, $s = 0.5$, and $L = 1.5$.

$k = w = C_0 = 0$. This originates from the fact that the nonlinear function $f(u)$ given by (3.1) is an odd function of u .

Next we explore the stability of the equilibrium solutions. By numerical simulations in Sec. II, we already know that it crucially depends upon the values of q and s , that is, equilibrium solutions become unstable through two different types of Hopf bifurcation such as in-phase and antiphase instabilities.

A. Wiggling motion

First we consider the stability of stationary interfaces under wiggling disturbances. To do it, we introduce deviations ξ^\pm as

$$X^\pm = \pm \frac{l}{2} + \xi^\pm, \quad (4.5)$$

where we set $\xi^+ = \xi^- = \xi$. The interface equation of motion obtained in Sec. III is linearized in terms of ξ . Note from (3.7a) and (3.8) that the deviations of C_0 and w vanish asymptotically. Hence Eq. (3.11) can be written up to $O(\xi)$ as

$$\frac{d\xi}{dt} = -2\delta v_I, \quad (4.6)$$

where we focus, without loss of generality, on only the right interface and hence δv_I is given by

$$\begin{aligned} \delta v_I = & \sum_{m=1}^{\infty} \delta C_{2m-1}(t) \cos \left[\frac{(2m-1)\pi \hat{l}}{L} \frac{\hat{l}}{2} \right] \\ & + \sum_{m=1}^{\infty} \frac{2\pi m}{L} C_{2m}^{(0)} \xi(t) \sin \left[\frac{2\pi m}{L} \frac{\hat{l}}{2} \right], \end{aligned} \quad (4.7)$$

with $\hat{l} = L - l$. An equation for $\delta C_n(t)$ is obtained from (3.7b) up to linear order of the deviation by

$$\begin{aligned} a(1-q) \frac{d\delta C_n}{dt} = & - \left[1 + \gamma + \left[\frac{\pi n}{L} \right]^2 \right] \delta C_n \\ & + \xi \gamma \frac{8}{L} \sin \frac{\pi n}{2} \sin \frac{\pi n l}{2L}. \end{aligned} \quad (4.8)$$

Because of the factor $\sin \pi n / 2$ in the last term, $\delta C_n(t)$ is finite only for odd integers, as has been incorporated in Eq. (4.7). Putting ξ and $\delta C_n(t) \propto \exp(\lambda t)$ in (4.6)–(4.8), we obtain the growth rate $\lambda (\neq 0)$ as

$$\begin{aligned} \lambda = & -\frac{16\gamma}{L} \sum_{m=1}^{\infty} \left\{ \frac{\left[\cos \left[\frac{\pi \hat{l}}{2L} (2m-1) \right] \right]^2}{a(1-q)\lambda + 1 + \gamma + \left[\frac{\pi(2m-1)}{L} \right]^2} \right. \\ & \left. - \frac{\left[\sin \left[\frac{\pi \hat{l}}{L} m \right] \right]^2}{1 + \gamma + \left[\frac{2\pi m}{L} \right]^2} \right\}. \end{aligned} \quad (4.9)$$

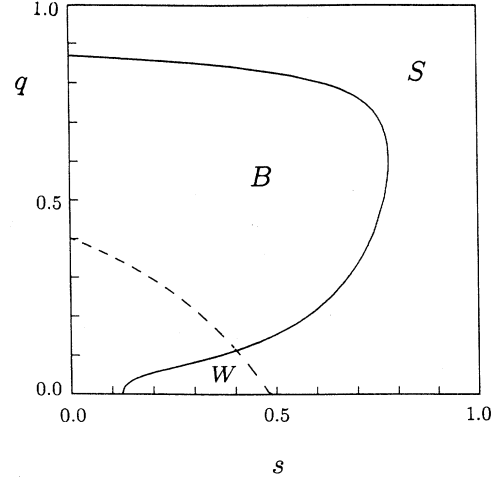


FIG. 11. Phase diagram obtained by the linear stability analysis of the interface equations of motion. The full line is the Hopf bifurcation threshold for breathing instability whereas the dashed line is that for wiggling instability. The parameters have been chosen as $a = 18.0$, $r = 1.5$, $l = 0.75$, and $L = 1.5$.

Equation (4.9) has been solved numerically for $l/L = \hat{l}/L = \frac{1}{2}$ truncated the summation at $m = 50$. The stability threshold where the real part of λ vanishes is plotted by a dashed line in Fig. 11. The imaginary part is always finite so that a Hopf bifurcation occurs on the line. In the region marked by W , one has a wiggling motion of domains.

B. Breathing motion

In order to examine the possibility of breathing motion, we have carried out the stability analysis by setting $\xi^+ = -\xi^- = \xi$. Equation for ξ is given, in this case, by

$$\frac{d\xi}{dt} = -2(\delta v_I + \delta w), \quad (4.10)$$

where δv_I is obtained from (3.9) as

$$\begin{aligned} \delta v_I = & \delta C_0 + \sum_{m=1}^{\infty} \delta C_{2m}(t) \cos \left[\frac{2\pi m}{L} \frac{\hat{l}}{2} \right] \\ & + \sum_{m=1}^{\infty} \frac{2\pi m}{L} C_{2m}^{(0)} \xi(t) \sin \left[\frac{2\pi m}{L} \frac{\hat{l}}{2} \right]. \end{aligned} \quad (4.11)$$

Equations for δC_n and δw are obtained by linearizing (3.7) and (3.8), respectively, as

$$a(1-q) \frac{d\delta C_0}{dt} = -\{1 + \gamma\} \delta C_0 - r(1-s) \delta w + \frac{4}{L} \gamma \xi, \quad (4.12)$$

$$a(1-q)\frac{d\delta C_n}{dt} = - \left[1 + \gamma + \left(\frac{\pi n}{L} \right)^2 \right] \delta C_n + \xi \gamma \frac{8}{L} \cos \frac{\pi n}{2} \cos \frac{\pi n l}{2L}, \quad (4.13)$$

$$aq \frac{d\delta w}{dt} = -rs\delta C_0 - (1+rs)\delta w + \frac{4}{L}rs\xi. \quad (4.14)$$

Setting ξ , δC_n ($n=0,1,2,\dots$), and $\delta w \propto \exp(\lambda t)$ and after some manipulation, we obtain from (4.10)–(4.14)

$$\lambda = - \frac{8}{L} \frac{r + ar\lambda(q - 2qs + s)}{\{a(1-q)\lambda + 1 + \gamma\}(1 + aq\lambda + rs) - rs\gamma} - \frac{16}{L} \lambda \sum_{m=1}^{\infty} \left\{ \frac{\left[\cos \frac{\pi m \hat{l}}{L} \right]^2}{a(1-q)\lambda + 1 + \gamma + \left[\frac{2\pi m}{L} \right]^2} - \frac{\left[\sin \left[\frac{\pi \hat{l}}{L} m \right] \right]^2}{1 + \gamma + \left[\frac{2\pi m}{L} \right]^2} \right\}. \quad (4.15)$$

The bifurcation threshold where the real part of λ vanishes while the imaginary part remains finite has been evaluated numerically for (4.15) up to $m=50$ and is plotted by a full line in Fig. 11. In the region marked by **B**, the equilibrium solutions are unstable under in-phase disturbances.

Here we make several remarks about the phase diagram in Fig. 11 obtained by the linear stability analysis. First of all, we note that the two bifurcation lines intersect each other at the point indicated by a dot. We thus find the occurrence of a double Hopf bifurcation in the q - s plane. This causes generally complicated oscillatory motions of domains at postthreshold as shown in Secs. II and V. Second, the wiggling motion dominates the breathing motion for sufficiently small values of q . This can be understood as follows. For $q=0$, the model equations (1.2) reduce to (1.5), which describe electric glow discharge. In this limit, the spatial average of u causes an inhibitory effect. This makes a wiggling motion more favorable than a breathing motion because the total magnitude of u or the total area of excited domains in the former motion is almost time independent and zero especially for $l/L = \frac{1}{2}$. Finally, we have reentrant phenomenon by decreasing q with a fixed value of s . That is, for large values of q , equilibrium solutions are stable. Decreasing q , the breathing instability appears and then for a further decrease of q , equilibrium solution again become stable. This also originates from the self-inhibitory property of the activator u for small values of q .

V. SIMULATIONS OF THE INTERFACE DYNAMICS

In order to investigate the postthreshold behavior, we have carried out computer simulations of the interface equation of motion given by Eqs. (3.7)–(3.11). The parameters have been chosen as $L=1.5$, $l=0.75$, $r=1.5$, $k=0$, and $a=18.0$. These are close to those used in the simulations in Sec. II except for the value of a . This is because the left-hand side of Eq. (1.2a) has a multiplicative factor ε while that of Eq. (2.3a) does not. The factor ε can be eliminated by redefining the time scale. Hence the parameter a in Eq. (1.2a) corresponds to $a\varepsilon$ in Eq. (2.3a).

The number of Fourier components C_n is $n=30$. We have verified the accuracy of the results by simulations for $n=60$. The set of ordinary differential equations (3.7)–(3.11) was solved numerically by the well-known Runge-Kutta-Gill method with the time increment 0.001.

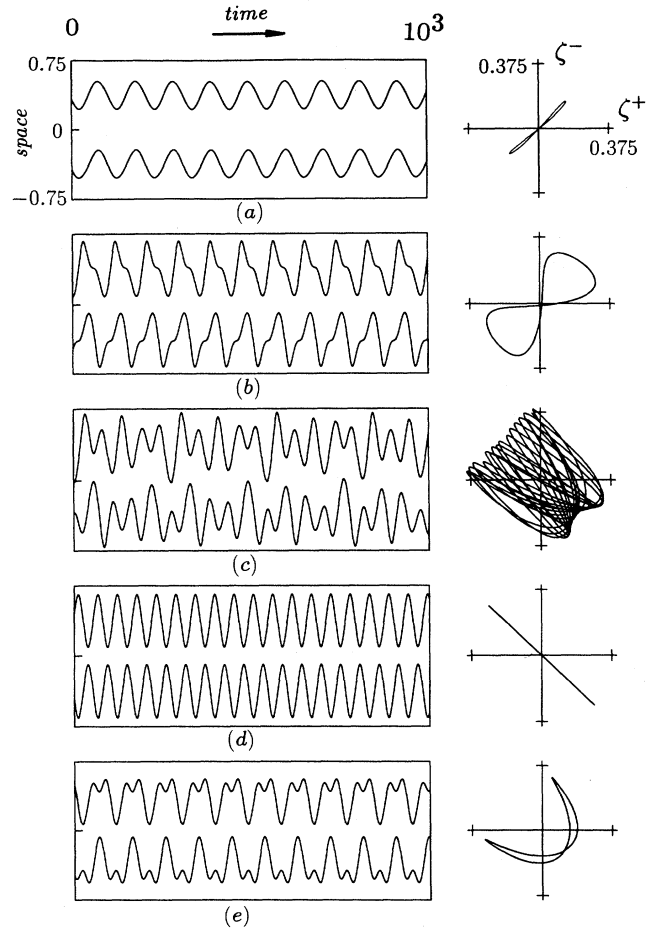


FIG. 12. Domain oscillations obtained from the interface equations of motion: (a) wiggling motion for $q=0.055$ and $s=0.41$; (b) distorted wiggling motion for $q=0.055$ and $s=0.12$; (c) quasiperiodic motion for $q=0.055$ and $s=0.0738$; (d) breathing motion for $q=0.055$ and $s=0.06$; (e) period-doubling oscillation for $q=0.2$ and $s=0.3$.

Figures 12 summarize the results of the simulations. These are the asymptotic results after eliminating initial transient. The figures on the left-hand side show the interface motions in the space- (vertical axis) time (horizontal axis) plane while those on the right-hand side plot the orbits in ζ_1 (horizontal) and ζ_2 (vertical) plane. Figure 12(a) is the typical wiggling motion obtained for $q=0.055$ and $s=0.41$. When one decreases s , the oscillation deviates from the sinusoidal curve and a phase difference between ζ_1 and ζ_2 appears. This can be clearly seen in Fig. 12(b) for $q=0.055$ and $s=0.12$. If one further decreases the value of s as $q=0.055$ and $s=0.0738$, one enters a quasiperiodic regime as in Fig. 12(c). Although not shown in the figure, we have verified that this is indeed quasiperiodic by a Lorentz map in the same manner as in Fig. 6. For slightly smaller values of s , a breathing motion appears as in Fig. 12(d), where $q=0.055$ and $s=0.06$. Note that the time and space scales are the same in all the figures. Thus the frequency of the breathing motion [Fig. 12(d)] is larger than that of the wiggling motion [Fig. 12(a)]. Figure 12(e) is an example of period-doubling oscillation. This emerges for $s=0.3$ and $q=0.2$. It is interesting to see that the main oscillation with lower frequency in Fig. 12(e) is a wiggling motion while the secondary oscillation is a breathing motion. Thus we note that the period doubling is a result of competition between these two fundamental motions.

The results shown in Fig. 12 are qualitatively consistent with those in Figs. 4–6 obtained by direct simulations of Eqs. (1.2) with a small but finite value of ϵ . One exception is the almost chaotic oscillation in Fig. 7. Although we carried out simulations in the q - s plane very carefully, we could not find any chaotic behaviors in the solutions of the interface equation of motion.

VI. CONCLUDING REMARKS

What we have shown in this paper is that multispecies activator and inhibitor systems exhibit a variety of spatiotemporal oscillating patterns compared with one-activator–one-inhibitor systems. To show the difference, we have studied pattern dynamics in a simple but non-trivial model of an interacting one-activator–two-inhibitor system given by Eqs. (1.2). Motions of excited domains have been investigated by both direct simulations and the interfacial approach. The global phase diagram for the oscillating instabilities has been drawn in q - s space. When the value of s is small, the system reduces to the one-activator–one-inhibitor system that was studied previously. It was predicted that an in-phase oscillation of domains is dominant for $l/L \approx \frac{1}{2}$ whereas an antiphase oscillation can appear for $l/L \ll 1$ [17]. Later, this property has also been studied in further detail by Ikeda and Nishiura [32].

For small values of q , the wiggling motion is the primary motion of domains. This is one of the characteristic features of the present system. Radehaus *et al.* [34] have obtained an antiphase oscillation in their numerical simulations of Eqs. (1.5), which is a particular case of Eqs. (1.2) with $q=0$. Thus their result is well consistent with the present analysis.

In the boundary region where the breathing and wiggling motions complete with each other, more complicated motions appear. In fact, computer simulations reveal several interesting spatiotemporal patterns such as period-doubling, quasiperiodic, and almost chaotic oscillations. However, their theoretical understanding is still in progress.

When we were preparing this manuscript, a paper by Niedernostheide *et al.* [36] was published. They also carried out computer simulations of the set of equations quite similar to Eqs. (1.5) and found breathing, wiggling, and quasiperiodic motions of a domain. However, the present study of the extended model Eqs. (1.2) is more general. Niedernostheide *et al.* considered only the particular limit of Eqs. (1.2), i.e., for $q=0$. One of the essential differences from their results is the existence of a double Hopf bifurcation point in the q - s plane as shown in Fig. 11. Almost chaotic oscillations, which were not obtained in Ref. [36], have been found near this point. Furthermore, we have applied the interfacial method to draw the precise stability diagram.

In this paper, we were restricted to dynamics of solutions with two internal layers. Of course, multilayer dynamics is also interesting, as shown in Fig. 13, which was obtained by the simulations of Eqs. (1.2) and where three different types of pattern of four-layer dynamics are shown. These results suggest that more variety of oscilla-

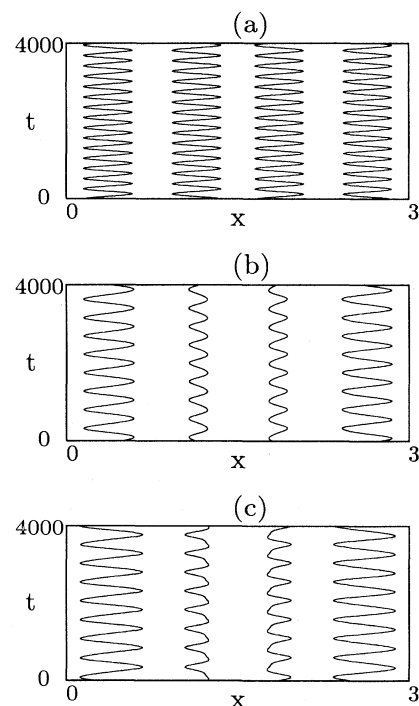


FIG. 13. Three different types of motions in four-layer dynamics of Eqs. (1.2) for $s=0.5$ and (a) $q=0.4$, (b) $q=0.35$, and (c) $q=0.3$. Other parameters are the same as in Fig. 4.

tion, which cannot be seen in the dynamics of the small number of layers as shown here and previously, is expected in an assembly of interacting excited domains. For this purpose, simulations of the partial differential equations such as (1.2) and the interface equation of motion are time consuming. A further coarse-grained approach, such as nonlinear coupled oscillators [37], would be more

useful. We hope to return to this problem elsewhere in the future.

ACKNOWLEDGMENT

This work was supported partly by the Grant-in-Aid of Ministry of Education, Science and Culture of Japan.

-
- [1] M. Cross and P. C. Hohenberg, *Rev. Mod. Phys.* **65**, 3 (1993).
- [2] E. Meron, *Phys. Rep.* **218**, 1 (1992).
- [3] A. N. Zaikin and A. M. Zhabotinsky, *J. Theor. Biol.* **40**, 45 (1973), and the earlier references cited therein.
- [4] A. T. Winfree, *Science* **175**, 634 (1972); **185**, 937 (1973).
- [5] J. D. Murray, *Mathematical Biology* (Springer, Berlin, 1989).
- [6] Q. Ouyang and H. L. Swinney, *Chaos* **1**, 411 (1991); K.-J. Lee, W. D. McCormick, J. E. Pearson, and H. L. Swinney, *Nature* **369**, 215 (1994).
- [7] J.-J. Perraud, K. Agladze, E. Dulos, and P. De Kepper, *Physica A* **188**, 1 (1992).
- [8] A. Turing, *Philos. Trans. R. Soc. London Ser. B* **237**, 32 (1952).
- [9] E. Schoell and D. Drasdo, *Z. Phys. B* **81**, 183 (1990).
- [10] F.-J. Niedernostheide, M. Arps, R. Dohmen, H. Willebrand, and H.-G. Purwins, *Phys. Status Solidi B* **172**, 249 (1992).
- [11] H. Willebrand, T. Hunteler, F.-J. Niedernostheide, R. Dohmen, and H.-G. Purwins, *Phys. Rev. A* **45**, 8766 (1992).
- [12] E. Ammelt, D. Schweng, and H.-G. Purwins, *Phys. Lett. A* **179**, 348 (1993).
- [13] L. Segel and J. L. Jackson, *J. Theor. Biol.* **37**, 545 (1972).
- [14] A. Gierer and H. Meinhardt, *Kybernetik* **12**, 30 (1972); H. Meinhardt, *Models of Biological Pattern Formation* (Academic, London, 1982); A. J. Koch and H. Meinhardt, *Rev. Mod. Phys.* **66**, 1481 (1994).
- [15] J. D. Murray, *Mathematical Biology* (Ref. [5]), p. 128.
- [16] S. Koga and Y. Kuramoto, *Prog. Theor. Phys.* **63**, 106 (1980).
- [17] T. Ohta, A. Ito, and A. Tetsuka, *Phys. Rev. A* **42**, 3225 (1990).
- [18] J. Rinzel and J. B. Keller, *Biophys. J.* **13**, 1313 (1973).
- [19] A. Ito and T. Ohta, *Phys. Rev. A* **45**, 8374 (1992).
- [20] J. J. Tyson and P. C. Fife, *J. Chem. Phys.* **73**, 2224 (1980).
- [21] R. May, *Stability and Complexity in Model Ecosystems* (Princeton University Press, Princeton, 1973).
- [22] J. J. Tyson and J. P. Keener, *Physica D* **32**, 327 (1988).
- [23] M. Mimura and Y. Kan-on, in *Patterns and Waves*, edited by T. Nishida *et al.* (North-Holland, Amsterdam, 1986).
- [24] T. Ikeda and M. Mimura, *J. Math. Biol.* **31**, 215 (1993).
- [25] Here we are concerned with multicomponent activator-inhibitor systems. There are, of course, a number of studies of multicomponent systems that are not an activator-inhibitor type. One example is found in A. L. Kawczynski, *J. Non-Equilib. Thermodyn.* **3**, 29 (1978), where a domain oscillation is modeled by a three-component system. However, two of the three variables constitute a harmonic oscillator, which are coupled to the third variable so that a domain oscillation occurs. We emphasize that this is entirely different from the mechanism of domain oscillations discussed in the present paper.
- [26] A. B. Rovinsky and M. Menzinger, *Phys. Rev. Lett.* **72**, 2017 (1994). In this paper, the authors show that a homogeneous steady solution in a three-component reaction-diffusion equation without an unstable subsystem is destabilized by a differential flow of one of the components. They call the unstable variable in the subsystem an activator and claim that the presence of an activator is a necessary condition for the diffusive (Turing) instability. This definition of an activator is consistent with ours as long as the diffusive instability is supercritical. In fact, the second statement concerning the necessary condition is valid only for a supercritical bifurcation because their analysis is a linear stability around a homogeneous solution. In the present paper, we are concerned with a nonuniform state that appears as a subcritical bifurcation in both monostable and bistable conditions.
- [27] V. S. Zykov, *Biophysics* **25**, 906 (1980); P. C. Fife, in *Non-equilibrium Dynamics in Chemical Systems*, edited by C. Vidal and A. Pacault (Springer, Berlin, 1984); J. P. Keener, *SIAM J. Appl. Math.* **46**, 1039 (1986).
- [28] Y. Nishiura and M. Mimura, *SIAM J. Appl. Math.* **49**, 481 (1989).
- [29] T. Ohta, M. Mimura, and R. Kobayashi, *Physica D* **34**, 115 (1989).
- [30] B. S. Kerner and V. V. Osipov, *Usp. Fiz. Nauk* **157**, 20 (1989) [*Sov. Phys. Usp.* **32**, 101 (1989)].
- [31] B. S. Kerner and V. V. Osipov, *Usp. Fiz. Nauk* **160**, 1 (1990) [*Sov. Phys. Usp.* **33**, 679 (1990)].
- [32] T. Ikeda and Y. Nishiura, *SIAM J. Appl. Math.* (to be published).
- [33] T. Ohta and M. Mimura, in *Formation, Dynamics and Statistics of Patterns*, edited by K. Kawasaki *et al.* (World Scientific, Singapore, 1990).
- [34] C. Radehaus, R. Dohmen, H. Willebrand, and F.-J. Niedernostheide, *Phys. Rev. A* **42**, 7426 (1990).
- [35] J. Rinzel and D. Terman, *SIAM J. Appl. Math.* **42**, 1111 (1982).
- [36] F.-J. Niedernostheide, R. Dohmen, H. Willebrand, B. S. Kerner, and H.-G. Purwins, *Physica D* **69**, 425 (1993).
- [37] T. Ohta and H. Nakazawa, *Phys. Rev. A* **45**, 5504 (1992).